

# Sub-Shotnoise Atomic Magnetometry

JM Geremia,\* John K. Stockton, and Hideo Mabuchi  
*Physics and Control & Dynamical Systems, California Institute of Technology, Pasadena CA 91125*  
(Dated: December 2, 2024)

We demonstrate sub-shotnoise sensitivity to an external magnetic field with a broadband atomic magnetometer. Our experiment utilizes spin-squeezing generated by continuous quantum nondemolition measurement and real-time feedback to achieve optimal rejection of multiplicative modeling uncertainties such as shot-to-shot atom number variation.

PACS numbers: 07.55.Ge, 03.65.Ta, 42.50.Lc, 02.30.Yy

Atomic magnetometers estimate the magnitude of an external magnetic field by observing Larmor precession in a polarized atomic sample [1]. This technique capitalizes on the relative ease of roughly orienting  $N \gg 1$  individual atomic dipoles along a common direction in space via optical pumping. For atoms with intrinsic spin angular momentum,  $\hbar f$ , such a sample displays a bulk magnetization,  $\mathbf{F}$ , oriented along the polarization axis with magnitude,  $\hbar\sqrt{F(F+1)} \approx \hbar F$ , where  $F = Nf$ .

Magnetometry is performed by polarizing the atoms along the laboratory  $x$ -axis, such that  $\mathbf{F}(0) = F\hat{\mathbf{x}}$ . In the presence of an external magnetic field  $\mathbf{b} = B\hat{\mathbf{y}}$  (assumed to lie along the  $y$ -axis),  $\mathbf{F}$  precesses,

$$\dot{\mathbf{F}}(t) = -\gamma\mathbf{F}(t) \times \mathbf{b}, \quad (1)$$

with Larmor frequency  $\omega_L = \gamma B$ . These dynamics confine the atomic magnetization to the  $xz$ -plane and the  $z$ -component of  $\mathbf{F}$  evolves from its initial value,  $F_z(0)$ , according to  $F_z(t) = F \exp(-t/T_2) \sin(\omega_L t)$ , with atomic coherence time,  $T_2$ . Given some experimental estimate,  $\tilde{F}_z$ , of  $F_z$  at time  $\tau$ , the corresponding field estimate is,

$$\tilde{B}(\tau) = \left[ \frac{\tilde{F}_z(\tau) - F_z(0)}{\gamma F \tau} \right] \approx \frac{\tilde{F}_z(\tau)}{\gamma F \tau}, \quad \tau \ll \omega_L^{-1}, T_2 \quad (2)$$

in the small Larmor precession, small decoherence limit.

Estimation uncertainty in  $\tilde{B}(\tau)$  results from the non-commutativity of the quantum operators,  $\hat{F}_x$ ,  $\hat{F}_y$  and  $\hat{F}_z$ , associated with the cartesian components of  $\mathbf{F}$ , which are subject to the Heisenberg uncertainty relation,  $\Delta\hat{F}_y\Delta\hat{F}_z \geq |\langle\hat{F}_x\rangle|/2$ . Thus, the atomic magnetization cannot be perfectly aligned along the  $x$ -axis, and an ensemble of similarly prepared atomic samples displays a distribution over initial values of  $F_z$  with mean  $\langle\hat{F}_z\rangle$  and variance  $\Delta\hat{F}_z^2 \equiv \langle\hat{F}_z^2\rangle - \langle\hat{F}_z\rangle^2$ . Assuming that  $F_z(0) = \langle\hat{F}_z(0)\rangle = 0$  introduces a quantum mechanical uncertainty into Eq. (2) of order  $\Delta\hat{F}_z$ , which in the absence of inter-atomic correlations (i.e., entanglement) is given by the coherent spin state value of  $\Delta\hat{F}_z^2 = F/2$ . The resulting estimation error,

$$\Delta\tilde{B}_{\text{SN}}(\tau) = \frac{\Delta\hat{F}_z(0)}{\gamma F \tau} = \frac{1}{\gamma \tau \sqrt{2F}}, \quad (3)$$

is known as the *shotnoise magnetometry limit* [2, 3].

We have recently shown [4, 5] that it is theoretically possible to surpass this limit using continuous quantum nondemolition (QND) measurement and the associated spin-squeezing [6, 7, 8]. Our procedure based on quantum Kalman filtering [9, 10] estimates the magnetic field from the average slope,  $y'(\tau)$ , obtained by linear regression of a continuous, noisy  $F_z$  measurement,

$$y(t) = F_z(t) + \zeta(t), \quad (4)$$

over the interval  $0 \leq t \leq \tau$ , where  $\zeta(t)$  reflects stationary noise (such as optical shotnoise). The resulting single-shot field estimate is given by,

$$\tilde{B}(\tau) = \frac{y'(\tau)}{\gamma F}, \quad \tau \ll \omega_L^{-1}, T_2 \quad (5)$$

with an uncertainty,  $\Delta\tilde{B}$ , due to the regression error.

Fig. 1 illustrates this procedure. Beginning from a coherent state at  $t = 0$ , the measurement reveals both the slope due to (small angle) Larmor precession and an offset due to the initial uncertainty in the orientation of  $\mathbf{F}$ . This offset is randomly distributed with variance  $F/2$  in an ensemble of measurement trajectories, and sub-shotnoise sensitivity results from the freedom to absorb the non-zero value of  $F_z(0)$  into the regression intercept, rather than the slope. This *quantum filtering* process minimizes the impact of  $\zeta(t)$  and  $\Delta\hat{F}_z(0)$  on field estimation and exploits the conditional spin-squeezing associated with continuous measurement [4] (provided that  $y(t)$  displays higher signal to noise in a  $1/\tau$  bandwidth than the coherent state uncertainty,  $\Delta\hat{F}_z \propto \sqrt{N}$ ).

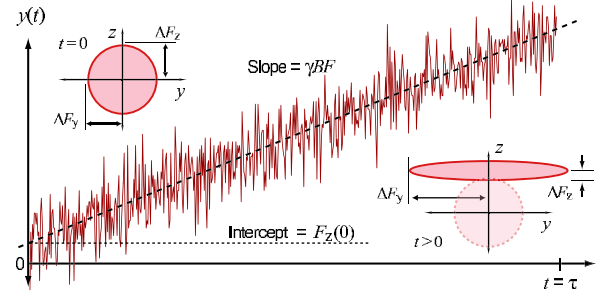


FIG. 1: Open-loop estimation procedure for sub-shotnoise magnetometry utilizing spin-squeezing generated by continuous measurement.

Experimentally, however, such an estimation procedure is hindered because it requires precise knowledge of the magnitude of the atomic magnetization—the field estimate in Eq. (5) explicitly divides the slope,  $y'(\tau)$ , by the value of  $F$ . Shot-to-shot variation in  $N$  produces fluctuations,  $\Delta F$ , in the length of  $\mathbf{F}$  that directly propagate into the field estimation as a proportional error,  $\Delta\hat{B}_F = y'\Delta F/(\gamma F) \approx B(\Delta F/F)$ . While atom number fluctuations introduce essentially no error when  $B = 0$  (and thus  $y'$  is zero), they can completely mask any improved resolution provided by spin-squeezing for  $B \neq 0$ .

To alleviate complications from atom number uncertainty, our magnetometer is implemented according to the closed-loop methodology [5, 11] illustrated in Fig. 2. The atomic sample is probed by a continuous QND  $F_z$  measurement provided by Faraday polarimetry [7, 8, 12] and the resulting photocurrent,  $y(t)$ , drives a high-precision  $y$ -axis magnet via negative feedback to stabilize  $F_z$  to zero. In the presence of an external magnetic field, the controller imposes a compensating field,  $\mathbf{b}_c(t) \simeq -B(t)\hat{\mathbf{y}}$  to prevent the atomic magnetization from precessing out of the  $xy$ -plane. The magnetic field is estimated from the time-averaged feedback signal,

$$\tilde{B}(\tau) = -\overline{B_c(t)}, \quad 0 \leq t \leq \tau \quad (6)$$

rather than the photocurrent. Since the magnetometer operates with  $F_z = 0$ , the closed-loop estimation is reasonably immune to atom number fluctuations.

We have recently demonstrated our capability to prepare spin-squeezed cold atom samples and to implement real-time quantum-limited feedback with an apparatus similar to that in Fig. 2 [13]. Our spin system is provided by the  $6^2S_{1/2}(F=4)$  ground state hyperfine manifold in  $^{133}\text{Cs}$ . Cold atoms are obtained from

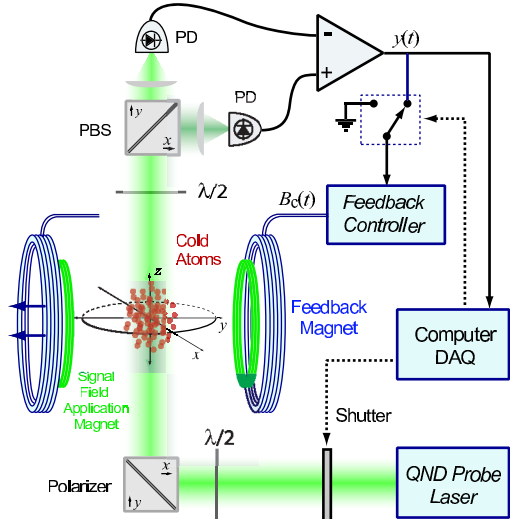


FIG. 2: Schematic of our apparatus for robust sub-shotnoise atomic magnetometry using real time quantum feedback, not including trapping, cooling and optical pumping optics as well as external coils for background magnetic field cancellation.

a  $10^{-8}$  Torr background vapor via standard laser cooling and trapping techniques. We reliably generate samples with  $N \sim 10^{11}$  at a temperature of  $T = 10 \mu\text{K}$  via a combination of magneto-optical trapping (MOT), dark spontaneous-force optical trapping (SPOT) and sub-doppler cooling. Shot-to-shot fluctuations in  $N$  are approximately 8%, with a systematic uncertainty (in fluorescence calibration)  $<20\%$ . Optical trapping beams (35 mW each, 2.5 cm diameter) are derived from an injection-locked diode laser. Coherent spin states along the laboratory  $x$ -axis are produced by optically pumping the atomic sample with circularly polarized light (100  $\mu\text{W}$  with a 9 mm Gaussian waist) tuned to the  $6^2\text{S}_{1/2}(F=4) \rightarrow 6^2\text{P}_{3/2}(F'=4)$  hyperfine transition.

Continuous QND measurement of  $F_z$  is implemented with a diode laser blue-detuned from the  $(F=4) \rightarrow (F'=5)$  transition by  $\Delta=550$  MHz. The 50  $\mu\text{W}$  probe beam is linearly polarized by a high extinction Glan-Thompson prism and Faraday rotation of the probe light is detected by a balanced polarimeter (1 MHz detector bandwidth) constructed from a high extinction Glan-Thompson beam splitter. The DC-coupled polarimeter photocurrent,  $y(t)$ , is of the form in Eq. (4) [11, 12].

In closed-loop configuration,  $y(t)$  programs a current supply that drives a  $y$ -axis Helmholtz coil via proportional feedback with 920 kHz bandwidth (limited by the current driver response). This magnetic field can be adjusted over  $\pm 50 \mu\text{G}$  to actuate the value of  $F_z$  by  $y$ -axis Larmor precession. A computer records the polarimeter output (with 5 MHz bandwidth), enables/disables the QND measurement by controlling a shutter on the probe laser (with 100 ns resolution), and opens/closes the feedback loop. A separate  $y$ -axis Helmholtz coil is used to produce the “signal” fields for detection.

Background magnetic fields were precisely nulled by minimizing residual Larmor precession, using a combination of large (1 m) external three-axis Helmholtz coils and smaller computer controlled trim-coils. We estimate that the resulting shot-to-shot field fluctuations (rms in a 100  $\mu\text{s}$  measurement window) were  $\sim 0.1 \mu\text{G}$ . Atomic decoherence was measured via Faraday spectroscopy to be  $< 6\%$  over the  $t = 100 \mu\text{s}$  measurement trajectories we consider. Further characterization of our coherent state preparation, atom number, transverse spin relaxation, spin-squeezing, and quantum noise limited feedback performance can be found in Ref. [13].

We began our experiment by initially operating the magnetometer with feedback disabled in order to characterize the adverse effects of shot-to-shot atom number fluctuations. Fig. 3 shows example open-loop field estimations performed using the procedure in Eq. (5) for two different magnetic fields,  $B = 0$  and  $B = 0.30 \mu\text{G}$  [14]. The Faraday polarimeter photocurrent in Fig. 3(a) for  $B = 0$  highlights many of the sub-shotnoise magnetometry issues described above. When the QND measurement is initiated at  $t = 0$  by opening the probe laser shutter,

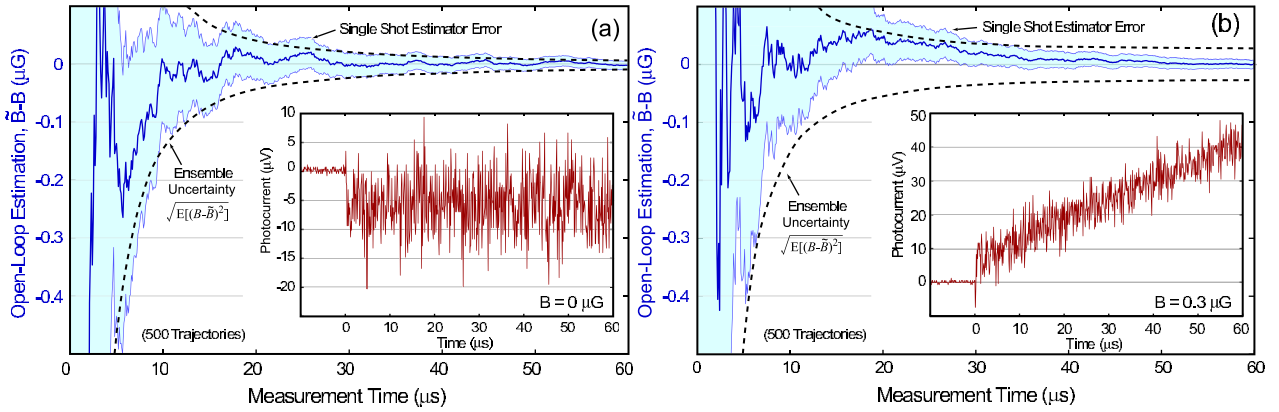


FIG. 3: Open-loop magnetic field estimation,  $\tilde{B} - B$ , as a function of measurement time for (a)  $B = 0$  and (b)  $B = 0.30 \mu\text{G}$ . Inset plots show the Faraday polarimeter photocurrent for each QND measurement trajectory.

the photocurrent establishes an average offset that is randomly distributed in an ensemble of similar trajectories. Our ability to observe this random offset reflects sufficient signal to noise in our polarimetry measurement to resolve the coherent state uncertainty,  $\Delta \hat{F}_z = \sqrt{F/2}$ , and thus to produce squeezing [4, 13].

Since  $B = 0$  in Fig. 3(a), the atoms do not undergo Larmor precession and the slope of  $y(t)$  is expected to be  $y' = 0$ . However, optical noise produces statistical fluctuations in  $y(t)$ ; the slope must be obtained by filtering (such as regression) to reduce the stationary noise by time-averaging. This procedure is demonstrated by the single-shot estimation trajectory for  $B = 0$  [dark solid line in Fig. 3(a)] computed according to Eq. (5) using the slope,  $y'(\tau)$ , obtained by linear regression of  $y(t)$  for  $0 \leq t \leq \tau$  and assuming  $N = 10^{11}$  atoms. The light shaded region denotes the single-shot estimator uncertainty,  $\Delta \tilde{B}$ , computed from the  $1-\sigma$  regression uncertainty and the dotted lines indicate the ensemble average field uncertainty, computed as  $\sqrt{E}[(\tilde{B} - B)^2]$  from 500 QND trajectories. Both the ensemble and single-shot

uncertainties converge to the same value for  $B = 0$ .

In sharp contrast, the ensemble uncertainty for the  $B = 0.30 \mu\text{G}$  estimation in Fig. 3(b) is substantially larger than the single shot estimator error (shaded region) computed using  $N = 10^{11}$ . Despite a clearly visible photocurrent offset, indicating the presence of spin-squeezing, the definitively non-zero slope is susceptible to uncertainty in the magnitude of  $\mathbf{F}$ . This point is further illustrated by the open loop ensemble estimation errors in Fig. 4. The dotted line indicates the shotnoise magnetometry limit computed from Eq. (3), with  $N = 10^{11}$  and conservatively assuming perfect optical pumping. While the  $B = 0$  ensemble uncertainty lies below the shotnoise limit for longer measurement durations, the uncertainty saturates to the appropriate atom-number fluctuation limit for  $B \neq 0$  (dotted lines indicate the expected uncertainty for  $\Delta N = 8\%$ ). For non-zero fields, the estimation uncertainty is worse than the shotnoise limit.

We then performed our closed-loop estimation procedure by enabling the feedback loop for the entire duration of each QND trajectory. The photocurrent in Fig. 5(a) displays no discernable slope despite the presence of a  $B = -0.30 \mu\text{G}$  field as the feedback loop drives a cancellation field [Fig. 5(b)],  $B_c$ , to maintain  $F_z = 0$ . The closed-loop field estimation, computed according to Eq. (6) for  $0 \leq t \leq \tau$ , is seen to be robust to atom number fluctuations—it is evident from Fig. 5(c) that the ensemble uncertainty (dotted lines) and single shot estimation error (shaded region) converge to the same value. This point is further emphasized in Fig. 4 where the closed-loop procedure clearly outperforms the shotnoise limit for all tested signal fields. Our closed loop magnetometry procedure is readily extended to detect time-dependent fields, as illustrated by Fig. 6. Here the estimated field is obtained by boxcar averaging the feedback signal over 1  $\mu\text{s}$  windows, corresponding to a measurement bandwidth  $\sim 1 \text{ MHz}$ . The inset compares the ensemble uncertainty,  $\sqrt{E}[(\tilde{B}(t) - B(t))^2]$ , calculated for each time-window to the corresponding shotnoise limit for a 1 MHz bandwidth

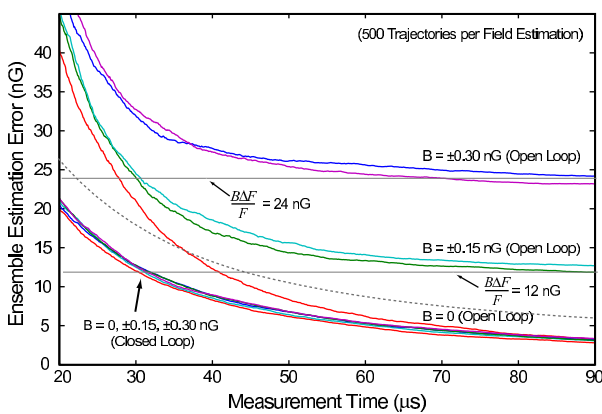


FIG. 4: Comparison of open and closed-loop field estimation uncertainties,  $\sqrt{E}[(B - \tilde{B})^2]$ . The dotted line reflects the theoretical shotnoise limit, Eq. (3), computed for  $\gamma = 2.19 \times 10^6 \text{ rad/G}\cdot\text{s}$  and  $F = 4 \times 10^{11}$ .

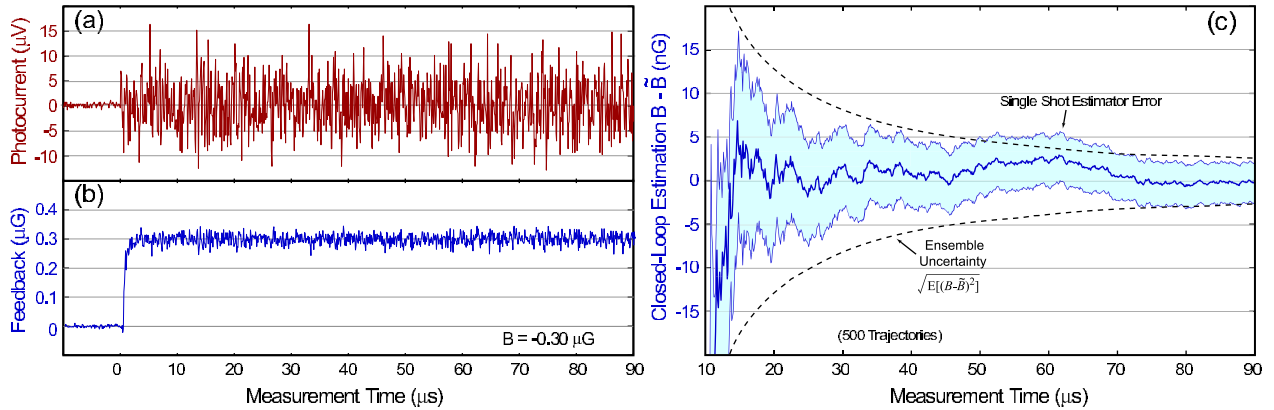


FIG. 5: (a) Closed-loop photocurrent for a  $B = -0.30 \mu\text{G}$  field, (b) real-time feedback field and (c) the resulting closed-loop field estimation,  $\hat{B} - B$ , as a function of measurement time.

[i.e., for  $\tau = 1 \mu\text{s}$  in Eq. (3)].

Our initial demonstration of sub-shotnoise magnetometry displays a field resolution of  $\sim 5 \text{ nG}$  in a  $90 \mu\text{s}$  estimation period, or an approximate sensitivity of  $\sim 5 \times 10^{-11} \text{ G} / \sqrt{\text{Hz}}$ . This value was limited by the maximum QND measurement strength that can be achieved with a free-space atom-probe coupling scheme. It would be possible to greatly improve the magnetometer resolution by employing an optical cavity and phase quadrature homodyne interferometry [11] to increase the degree of spin squeezing. Currently accessible technology in experimental cavity QED would permit sub-shotnoise magnetometers of this type to achieve better than  $1 \text{ fT}$  [15] resolution in a  $100 \text{ kHz} - 1 \text{ MHz}$  bandwidth, approaching  $1 \text{ aT} / \sqrt{\text{Hz}}$  sensitivity [4].

These results highlight what we anticipate to become a central theme in quantum-limited metrology. Feedback enables a precision measurement to achieve optimal insensitivity to classical uncertainty without sacrificing resolution [5, 16]. Such an approach is likely to be essential

for obtaining acceptable performance in various applications including spin resonance measurements, atomic frequency standards, and matter-wave gravimetry. This work was supported by the NSF (PHY-9987541, EIA-0086038), the ONR (N00014-00-1-0479), and the Caltech MURI Center for Quantum Networks (DAAD19-00-1-0374). JKS acknowledges a Hertz fellowship. We thank Andrew Berglund, Michael Armen, Andrew Doherty and Vladan Vuletic for helpful discussions.

\* Electronic address: jgeremia@Caltech.EDU

- [1] J. Dupont-Roc, S. Haroche, and C. Cohen-Tannoudji, Phys. Lett. A **28**, 638 (1969).
- [2] D. Budker, et al., Rev. Mod. Phys. **74**, 1153 (2002).
- [3] Our assumption that  $t \ll T_2$  permits a direct comparison between Eq. (3) and the expression in Ref. [2].
- [4] J. Geremia, J. K. Stockton, A. C. Doherty, and H. Mabuchi, Phys. Rev. Lett. **91**, 250801 (2003).
- [5] J. K. Stockton, J. Geremia, A. Doherty, and H. Mabuchi, Phys. Rev. A., accepted (2003), quant-ph/0309101.
- [6] M. Kitagawa and M. Ueda, Phys. Rev. A **47**, 5138 (1993).
- [7] A. Kuzmich, L. Mandel, and N. P. Bigelow, Phys. Rev. Lett. **85**, 1594 (2000).
- [8] B. Julsgaard, A. Kozhekin, and E. S. Polzik, Nature **413**, 400 (2001).
- [9] V. P. Belavkin, Rep. on Math. Phys. **43**, 405 (1999).
- [10] H. Mabuchi, Quantum Semiclass. Opt. **8**, 1103 (1996).
- [11] L. K. Thomsen, S. Mancini, and H. M. Wiseman, Phys. Rev. A **65**, 061801 (2002).
- [12] G. A. Smith, S. Chaudhury, and P. S. Jessen, J. Opt. B: Quant. Semiclass. Opt. **5**, 323 (2003).
- [13] J. Geremia, J. K. Stockton, and H. Mabuchi, submitted (2004).
- [14] Additional information and data analysis code is available at <http://minty.Caltech.EDU/Ensemble>.
- [15] I. K. Kominis, T. W. Kornack, J. C. Allred, and M. Romalis, Nature **422**, 596 (2003).
- [16] D. W. Berry and H. M. Wiseman, Phys. Rev. A **65**, 043803 (2002).

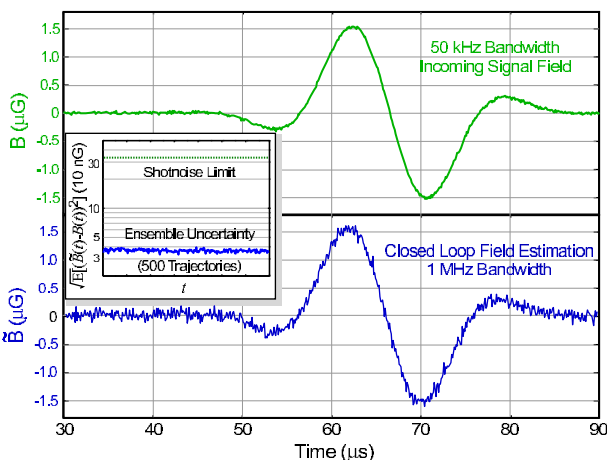


FIG. 6: Detection of a time-dependent magnetic field pulse with zero area using our closed-loop atomic magnetometry procedure.